Recoding a cocaine-place memory engram to a neutral engram in the hippocampus

Stéphanie Trouche[1], **Pavel V Perestenko**[1], **Gido M van de Ven**[1], **Claire T Bratley**[1], **Colin G McNamara**[1], **Natalia Campo-Urriza**[1], **S Lucas Black**[1], **Leon G Reijmers**[2], and **David Dupret**[1]

[1]Medical Research Council Brain Network Dynamics Unit, Department of Pharmacology, University of Oxford, Oxford, United Kingdom

[2]Department of Neuroscience, School of Medicine, Tufts University, Boston, MA, USA

Abstract

The hippocampus provides the brain's memory system with a subset of neurons holding a map-like representation of each environment experienced. We found in mice that optogenetic-silencing those neurons active in an environment unmasked a subset of quiet neurons, enabling the emergence of an alternative map. This intervention applied in a cocaine-paired environment neutralized an otherwise long-lasting drug-place preference, showing that recoding a spatial memory engram can alleviate associated maladaptive behavior.

Memory is central to behavior, enabling individuals to respond to their environment using past experiences[1]. The spatially-tuned and temporally-coordinated activity of hippocampal CA1 principal cells contributes to adaptive memories by providing the brain with neuronal engrams that represent the spatial context of life events[2–5]. Nonetheless, the recall of certain representations, such as those associating an environment with a drug of abuse, can impair the individual's ability to make adaptive choices, including an uncontrolled drive to revisit drug-paired locations[6]. Manipulating hippocampal neuronal representations could redress undesirable spatio-contextual behaviors. However, a given hippocampal 'place cell' can contribute not to one but to multiple representations[4,7–12]. Therefore, it remains unknown how the hippocampal neuronal representation of a particular place could be selectively edited. In a given environment the hippocampus exhibits, alongside the active place cells, a subset of quiet neurons without clear spatial selectivity[3,9,12–17]. Here, we used a *c-fos*-based optogenetic approach to silence hippocampal neurons active in a particular environment and examined whether quiet neurons could implement an alternative representation that neutralizes a drug-place memory.

To label and manipulate hippocampal neurons recruited during exploration of an environment, we bilaterally injected the dorsal CA1 of c-fos-tTA transgenic mice with a TRE3G-ArchT-GFP viral construct (Fig. 1a and Supplementary Fig. 1). In these c-fos::ArchT mice neuronal activation leads to the expression of the tetracycline transactivator (tTA) through the promoter of the *c-fos* immediate early gene. The transient removal of doxycycline (Dox) from the mouse diet enables the tTA to interact with the tetracycline-responsive element (TRE3G), thereby tagging active neurons with the light-driven silencer Archaerhodopsin-T (ArchT). To test this tagging procedure, a first group of mice explored a circular-walled enclosure (the 'circle') while transiently off Dox (Fig. 1b). In these 'tagged mice', 6.28±0.38% of neurons in the CA1 pyramidal cell layer expressed ArchT-GFP of which 99.70±0.10% were pyramidal cells ('tagged neurons'; Fig. 1c; n=4 mice). This neuronal tagging lasted at least six days (n=2 mice; Supplementary Fig. 1b) and was virtually absent in c-fos::ArchT control mice (n=3) always fed on Dox (0.09%±0.02%, P<0.001 tagged versus control; Fig. 1a-c).

We next optogenetically silenced ArchT-GFP-tagged neurons while monitoring CA1 ensemble activity from c-fos::ArchT tagged mice (n=5; Fig. 1a,b). Tagged mice were transiently taken off Dox to tag CA1 neurons in the circle (Fig. 1b; Day 0), and recordings were performed on the following days during re-exposure to the circle with CA1 light-delivery (561nm, 30s-light-ON pulses with 70s-light-OFF intervals; Fig. 1b). We found that ArchT photo-silencing significantly decreased the firing rate of 133 neurons ('putative tagged neurons'; OFF=1.08±0.08Hz, ON=0.06±0.005Hz) out of the 1,083 principal neurons recorded (range: 161–231 daily recorded neurons over 6 days) while increasing the firing rate of 332 neurons ('alternative neurons'; OFF=0.84±0.04Hz, ON=1.97±0.08Hz; Fig. 1d,e and Supplementary Fig. 2). The activity of the remaining 618 neurons was not significantly altered ('unchanged neurons'; Fig. 1d,e; OFF=0.70±0.04Hz, ON=0.78±0.04Hz). We did not observe such a light-induced firing switch amongst the 358 CA1 principal neurons recorded from c-fos::ArchT control mice continuously fed on Dox (n=2; Fig. 1b and Supplementary Fig. 2a,b).

We then sought to identify functional differences between tagged and alternative neurons. We found that the baseline (light-OFF) firing rate of alternative neurons was initially lower in the circle than that of tagged and unchanged neurons (Days 1–2; Fig. 2a and Supplementary Fig. 2d,e). In contrast, their firing rate matched that of the tagged and unchanged neurons during exploration of a square-walled enclosure mice also experienced each day (the 'square'; Supplementary Fig. 2d,e). This suggests that the preferred recruitment of a selected subset of neurons in a given environment is associated with tight inhibitory control over other principal cells[18]. Accordingly, the photo-evoked switch in activity of tagged and alternative neurons (Fig. 1e) was accompanied by a fine redistribution of interneuron firing activity, without a change in the interneuron population mean rate (n=189 interneurons recorded; Supplementary Figure 3).

During the following days, the baseline (light-OFF) activity of alternative neurons increased in the circle while that of tagged neurons concomitantly decreased (Fig. 2a), as revealed by the slope of the linear regression (firing rate = $\beta_0 + \beta_1 \times$ days; with $\beta_1 = 0.15$ and -0.19 for alternative and tagged neurons, respectively; both Ps<0.00001). In these tagged mice, there

was no similar rate shift of light-unresponsive neurons in the circle ('unchanged neurons', Supplementary Fig. 4a,b), nor for tagged and alternative neurons in the square (both Ps>0.19). Moreover, no shift in neuronal activity was observed in c-fos::ArchT tagged mice exploring the circle without CA1 light-delivery (n=3; Supplementary Fig. 4c,d). Thus, the repetitive photo-silencing of neuronal activity in the circle, but not context re-exposure *per se*, caused the tagged/alternative firing rate shift.

We next computed place firing rate maps in light-OFF and light-ON epochs. During the first days of re-exposure to the circle, tagged neurons but not alternative neurons exhibited clear light-OFF spatial firing fields (Fig. 2b,c and Supplementary Fig. 5). While light-delivery strongly disrupted the place fields of tagged neurons, it simultaneously led to the emergence of spatially-structured firing of alternative neurons (Fig. 2c and Supplementary Figs. 5b,c and 6). This photo-evoked switch from one hippocampal map to another was not observed in c-fos::ArchT control mice (Supplementary Figs. 7,8), ruling out non-specific remapping caused by light-delivery. Moreover, the hippocampal map photo-switch was associated with a transient increase in locomotor reactivity which diminished over the following days of light-delivery, suggesting that the expression of the alternative representation caused tagged mice to initially treat the circle as a new enclosure (Supplementary Fig. 8). Interestingly, concurrent with this behavioral shift the baseline spatial tuning of the alternative neurons increased while that of tagged neurons decreased (Fig. 2b,d and Supplementary Figs. 5,6; with $\beta_1 = 0.08$ and -0.07, respectively; both Ps<0.00001), but no such change was observed in light-unresponsive neurons (Supplementary Fig. 4b).

Information processing in cortical circuits is thought to rely on spiking activity coordinated over short-intervals in distributed groups of neurons forming assemblies[5]. We tested whether our intervention changed the contribution of tagged and alternative neurons to the temporal expression of hippocampal assemblies. We detected significant assembly-patterns from the co-fluctuation of (light-OFF) neuronal discharges in 25-ms windows, and described them by weight vectors representing the contribution of each neuron to each assembly-pattern (Fig. 2e and Supplementary Fig. 9a-f). We found that while tagged neurons predominantly contributed to assembly-pattern expression in the first 3-day block, this was reversed in the next 3-day block which was marked by the dominant contribution of their alternative peers (Fig. 2f) without a change in the average strength of assembly-activations (Supplementary Fig. 9g,h).

We finally investigated whether recoding a hippocampal map could reset the memory of an environment in which a drug had been previously experienced. Drugs of abuse, through their association with environmental cues and contexts, produce powerful and long-lasting memories that precipitate relapse[6]. Concordantly, we found that more CA1 neurons recruited in a cocaine-paired environment were re-activated during drug-free re-exposure to that environment than for a saline-paired environment (Supplementary Fig. 10). We thus tested whether our optogenetic intervention could revoke the memory of a cocaine-paired environment. We trained mice in a conditioned place preference task to learn the association of one compartment with cocaine and the other with saline, such that they expressed a cocaine-place preference (Fig. 3, Test 1). This cocaine-place association was long-lasting for both c-fos::ArchT control mice (n=8) and wild-type control littermates (n=8) (Fig. 3, Test 2).

However, c-fos::ArchT tagged mice (n=13) no longer exhibited a cocaine-place preference (Fig. 3 and Supplementary Fig. 11) after the repetitive CA1 photo-silencing in the cocaine-paired compartment had shifted neuronal activity from the tagged to the alternative subset (Supplementary Fig. 11c). The cocaine-place preference of tagged mice could not be reinstated in response to cocaine-priming injection, suggesting that the shift to the alternative hippocampal map had neutralized the cocaine-place memory (Supplementary Fig. 11d). However, both tagged and control mice were able to express a place preference for a never before experienced compartment (Supplementary Fig. 11e,f). We therefore propose that in tagged mice the absence of spatial preference after hippocampal map recoding indicates that the compartment previously paired with cocaine was no longer associated with the drug experience and yet was perceived as familiar again.

Previous studies using *c-fos*-based optogenetic technology have influenced the behavioral output of a spatio-contextual memory by altering the interaction the hippocampus has with extra-hippocampal circuits that attach valence to context[19,20]. In this study, we report an alternative approach that directly changes the hippocampal ensemble representation of a spatial context by disengaging the initially recruited neurons while enabling previously quiet neurons to emerge and provide an alternative representation. Drug-paired spatio-contextual memories increase the propensity for relapse in cocaine users and prompt drug-seeking behavior in laboratory rodents[6]. Here, our approach for editing the hippocampal ensemble representing an environment associated with cocaine was able to revoke drug-induced spatial preference in mice. In contrast with regular extinction, the neutralizing effect of this intervention was not overturned by a priming cocaine experience. Together, our data demonstrate that recoding a selective hippocampal engram represents a potent strategy to reset spatial memories and neutralize maladaptive behavior.

ONLINE METHODS

Subjects

c-fos-tTA animals were adult transgenic mice heterozygous for the transgene carrying the *c-fos* promoter-driven tetracycline transactivator (tTA)[21]. Mice were bred from c-fos-tTA mice crossed with C57Bl6/J mice, and housed with their littermates until used in the experimental procedure. Food containing doxycycline (the "regular Dox"; 40mg/kg Dox chow; Bio-Serv) was provided for at least two weeks before the injection surgery. c-fos-tTA-LacZ animals[22] were adult male double transgenic mice carrying the tetracycline transactivator (tTA) transgene under the control of the *c-fos* promoter, as well as a second transgene linking the *tetO* promoter to the tau-LacZ reporter and the tetracycline transactivator mutant tTA^H100Z (tTA*) in order to maintain the tetO-linked gene expression after the initial neuronal activation. In the absence of doxycycline the active *tetO* promoter forms a positive feedback loop with tTA* that then becomes doxycycline insensitive. The c-fos-tTA-LacZ mice were backcrossed to a C57Bl6/J background and were raised on food with regular Dox. These two c-fos-tTA mouse lines were generated at The Scripps Research Institute and maintained at Tufts University until shipment to the MRC BNDU at the University of Oxford. Mice had free access to food and water *ad libitum* in a dedicated housing room with a 12/12h light/dark cycle (7am-7pm). Behavioral experiments were performed during daylight. All

experiments involving animals were conducted according to the UK Animals (Scientific Procedures) Act 1986 under personal and project licenses issued by the Home Office following ethical review.

Viral construct cloning, packaging and testing

The pAAV-TRE3G-ArchT-GFP plasmid was constructed using the pAAV-CamKII-ArchT-GFP backbone vector (Addgene plasmid # 37807)[23] where the original *CamKII* promoter was substituted, using PacI and the BamHI restriction enzymes recognition sites, with the third generation of tetracycline responsive element containing promoter (TRE3G, Clontech Laboratories, Inc.). The recombinant AAV vector was serotyped and packaged with AAV_2 coat proteins (University of North Carolina). Dox-controlled transcriptional activation of ArchT-GFP expression was first assessed in cultured HEK-293 cells (Supplementary Fig. 1a) co-transfected with a pTet-DualOFF vector (Clontech Laboratories Inc.; IRES2-ZsGreen1 cassette removed using EcoRI and HindIII restriction sites followed by Klenow fragment blunting and self-ligation of the vector). The ArchT-GFP expression was assessed in c-fos-tTA mice injected in the CA1 region of the dorsal hippocampus with the TRE3G-ArchT-GFP viral construct while under regular Dox (n=9 mice, Supplementary Fig. 1b). One month post injection, these c-fos::ArchT mice explored a circular-walled environment (the "circle", 43cm diameter, 26cm height) while either off Dox ("tagged mice", n=6; Dox removed from food diet three days before) or on Dox ("control mice", n=3). Both groups were put on food containing a high dose of Dox (1g/kg) immediately after exploration of the circle in order to block any further neuronal tagging and were returned to a regular Dox diet the following day. The mice were perfused three or six days later and their brain was extracted for immunohistochemistry procedures.

Surgical procedures

c-fos-tTA mice were bilaterally injected and implanted under deep anesthesia and analgesia[24]. TRE3G-ArchT-GFP viral vector injections (2×450nl for each side) were performed bilaterally in the dorsal CA1 using stereotaxic coordinates (−1.6mm and −2.4mm anteroposterior, ±1.7mm lateral from bregma and −1.1mm ventral from the brain surface). The viral vector was delivered at a rate of 100nl/min using a glass micropipette[24]. After two weeks of recovery mice were implanted with a ten-independently movable tetrode microdrive combined with two optic fibers (Doric lenses, Québec, Canada) targeting the dorsal CA1 bilaterally[24].

Recording procedures

Following the implant surgery, mice recovered for at least one week before familiarization to the recording procedure commenced. Mice were handled 5–10 minutes in a dedicated towel, twice a day, and connected to the recording system for 1–2h a day for at least a week. During this time, tetrodes were gradually lowered towards the pyramidal cell layer. All cell ensemble recordings were performed from the CA1 hippocampus of adult male mice. On recording days, each morning tetrodes were lowered into the pyramidal cell layer in search of multi-unit spiking activity as previously described[24]. All recordings were performed under dim light conditions (20–40lux) with no rewards provided. At the end of each recording day, tetrodes were raised to avoid damaging the pyramidal cell layer overnight.

The primary recordings completed in this study were from drug-free c-fos::ArchT tagged mice exploring the circle paired with CA1 light-delivery (see below) and a square-walled enclosure (the "square", 46cm×46cm×38cm; ~30min) without light-delivery (n=5 tagged "light-IN" mice). Wooden pieces were added on some of the square walls on each day to make it novel. In these drug-free experiments recordings were also performed from two control groups. The first control group consisted of c-fos::ArchT control (non-tagged) mice exploring the circle paired with light-delivery and the square without light-delivery (n=2 control "light-IN" mice) and the second control group consisted of c-fos::ArchT tagged mice exploring the circle without light-delivery and the square with light-delivery (n=3 tagged "light-OUT" mice). The purpose of light-delivery in tagged light-OUT mice was to allow the identification of tagged and alternative neurons without affecting their activity during re-exposure to the circle. Locomotor behavior of tagged light-IN mice was similar to that of both non-tagged light-IN and tagged light-OUT mice in the circle during baseline condition (distance travelled = 110.54±7.90m, 103.23±5.78m and 113.19±3.01m, respectively; animal speed = 5.26±0.38, 4.91±0.27 and 5.39±0.14; P=0.78). CA1 light-delivery in tagged light-IN mice was however initially associated with an increased locomotor reactivity, indicative of a behavioral novelty response to the expression of the alternative hippocampal map (see Supplementary Figure 8). In experiments involving cocaine, recordings were performed in mice (n=4 on C57Bl6 background) exploring an enclosure paired with a saline administration (0.9% saline, i.p) followed by the exploration of another enclosure paired with a cocaine administration (10mg/kg, i.p.; Sigma) (Supplementary Figure 11a). Additionally, in order to determine whether the shift in neuronal activity caused by the repetitive photo-silencing in the drug-free circle enclosure (Figure 2) also occurred in a cocaine-paired environment recordings were performed in c-fos::ArchT tagged mice (n=2) during the conditioned place preference task (Supplementary Figure 11c).

Doxycycline treatment

Tagged, but not control, c-fos::ArchT mice were taken off regular Dox three days before the tagging day (Day 0), a period during which familiarization to the recording procedure was temporarily discontinued for both tagged and control mice. On the tagging day of the drug-free open-field experiment both tagged and control c-fos::ArchT mice explored the circle for 45min. For the CPP experiment, the least preferred enclosure was identified for each mouse during the pre-test and that enclosure was paired with cocaine and explored for 45min on the tagging day (see *Conditioned place preference section* below). All mice went back to their home cage immediately after the tagging and were fed with high dose of Dox. The following day mice returned to the regular Dox diet.

Multichannel data acquisition

The signals from the electrodes were buffered on the head of the animal (unity gain op-amps, Axona Ltd, www.axona.com) and transmitted over a single strand of litz wire to a dual stage amplifier and band pass filter (gain 1000, pass band 0.1Hz to 5kHz; Sensorium Inc., Charlotte, VT)[24], or (in a second setup) the electrode signals were amplified, multiplexed, and digitized using a single integrated circuit located on the head of the animal (RHD2164, Intan Technologies, Los Angeles; pass band 0.09Hz to 7.60kHz). The amplified and filtered electrophysiological signals were digitized at 20kHz and saved to disk along

with the synchronization signals from the position tracking and the laser activation. In order to track the location of the animal three LED clusters were attached to the electrode casing and captured at 25 frames per second by an overhead color camera.

CA1 light-delivery

A 561nm diode pumped solid state laser (Laser 2000, Ringstead, UK) was used to deliver light to the dorsal CA1 (~15mW) of c-fos::ArchT tagged and control mice through two lengths of optic fiber and a rotary joint with splitter (Doric Lenses, Québec, Canada)[24]. For the drug-free open-field experiment, light was delivered in the circle ("light-IN") using trains of 30 pulses 30s in duration ("light-ON") with 70s between pulses ("light-OFF"). As these experiments relied on the propensity of the mice to spontaneously explore, this light-delivery protocol was chosen to ensure the mice evenly covered the circle in both light-OFF and light-ON epochs (i.e., ~35min and 15min total exploration, respectively). CA1 photo-silencing was also performed in c-fos::ArchT tagged mice during the exploration of the square, i.e. after that of the circle ("light-OUT"; 1s light pulses with 9s between pulses), in order to optogenetically identify tagged and alternative neurons. For the CPP experiment, trains of 30 light pulses of 30s duration were delivered during the 20 minute re-exposure sessions to the cocaine-paired enclosure. A 20-minute re-exposure session with light-delivery was used per day in the CPP experiment in order to prevent possible drug-conditioned memory extinction due to prolonged and non-reinforced context re-exposure to the cocaine-conditioned enclosure. Thus, shorter light-OFF (10s) intervals were used to preserve a total of 15-minute CA1 light-delivery.

Spike detection and unit isolation

The recorded signals were digitally band pass filtered (800Hz to 5kHz) offline for spike detection and unit isolation. Spikes were detected using a threshold in the RMS power (0.2ms sliding window) of the filtered signal. Unit isolation was performed on the first principal components calculated for each channel recorded by the tetrode in question. This was achieved by automatic over clustering to up to 100 clusters (KlustaKwik, klusta-team.github.com) followed by graphically-based manual recombination and further isolation informed by cloud shape in principal component space, cross-channel spike waveforms, auto-correlation histograms and cross-correlation histograms[24–26]. All sessions recorded on a given day were concatenated and cluster cut together to monitor cells throughout the day. Only well-isolated and stable units over the entire day were used for analysis[24] and hippocampal principal cells and interneurons were identified by their auto-correlogram, firing rate and spike waveform as described before[25]. Firing probabilities relative to theta oscillations and SWR events[25] were used to classify interneurons as established elsewhere[27–29]. A total of 1,083 principal cells (from Day 1 to 6: n=200, 161, 189, 139, 163 and 231, of which 28, 17, 18, 18, 22 and 30 tagged neurons; 62, 65, 71, 30, 25 and 79 alternative neurons; 110, 79, 100, 91, 116 and 122 unchanged neurons) and 189 interneurons were isolated from the CA1 hippocampus recordings of c-fos::ArchT light-IN tagged mice during drug-free exploration of open-field enclosures. The number of cells isolated from the other recordings is indicated where appropriate.

Identification of tagged and alternative neurons

Light-modulation of neuronal discharge was identified by calculating, for each neuron, the spike discharge across one-second time bins relative to light pulse onsets. The mean firing probability across bins during light-delivery was then compared to the mean across light-OFF bins. Neurons with a light-ON firing probability more than two standard deviations outside the light-OFF value were deemed to exhibit a significant light response. Neurons that were significantly photo-silenced were classified as 'putative' tagged neurons while those exhibiting a significant rate increase were classified as alternative neurons. Light-response scores (light-ON versus light-OFF firing rate difference over their sum) of tagged neurons and those of alternative neurons both had unimodal distributions (both Ps>0.76, Hartigan's Dip test; mean±s.e.m rate score: −0.82±0.01 and 0.44±0.01, respectively). Neurons with no light-modulated activity were grouped together as "unchanged neurons".

Spatial rate maps

The horizontal plane of the recording arena was divided into bins of approximately 2×2cm to generate spike count maps (number of spikes fired in each bin) for each unit and an occupancy map (time spent by the animal in each bin). All maps were then smoothed by convolution with a two-dimensional Gaussian kernel having standard deviation equal to one bin width. Finally, spatial rate maps were generated by normalizing the smoothed spike count maps by the smoothed occupancy map. Spatial coherence was calculated from the unsmoothed place rate maps; it reflects the similarity of the firing rate in adjacent bins, and is the z-transform of the Pearson correlation (across all bins) between the rate in a bin and the average rate of its eight nearest neighbors[30,31]. The inter-quartile range in spatial coherence of the population was 0.49–0.74. The population map similarity (Supplementary Figure 8d) was measured as previously described[24,30,32]. It compares all the place maps from two different time periods in a pairwise fashion and represents the degree to which cells that fired in similar regions of space (i.e., overlapping place fields) in one time period still fire in similar regions in the other time period. It is calculated by first computing the place field similarity (PFS) value for each cell pair during the first time period as the Pearson correlation coefficient from the direct bin wise comparisons between the spatial rate maps of the two cells limited to valid bins (occupancy greater than zero). This is repeated for the second time period and the population map similarity between the two time periods is calculated as the Pearson correlation coefficient between the PFS values from each of the time periods.

Principal cell assembly-patterns

To quantify the extent to which hippocampal principal cells contribute to the formation of neuronal assemblies by synchronizing their firing activity with peer neurons, significant co-firing patterns were detected using an unsupervised statistical method based on independent component analysis (ICA) (Figure 2e,f and Supplementary Fig. 9)[33]. Light-OFF epochs during exploration of the circle were divided into 25ms time-bins[34], and for every principal cell the number of spikes per bin was counted. Time windows matching theta-band (4–12Hz) oscillatory waves (~100ms) were also used as they represent another natural temporal division for the expression of hippocampal cell assemblies (Supplementary Fig. 9f). In order

to restrict the analysis to the temporal coordination of spiking activity without bias due to differences in the average firing rates, the binned spike-counts were normalized for each neuron by a z-score transform:

$$z_{i,b} = \frac{x_{i,b} - \mu_{x_i}}{\sigma_{x_i}}$$

where for neuron i, $Z_{i,b}$ is its z-scored spike-count in bin b, $x_{i,b}$ its spike-count in bin b, μ_{x_i} its mean spike-count across all bins and σ_{x_i} the standard deviation of its spike-counts. This set each neuron to have a null mean rate with unitary variance. With the number of principal cells denoted by n and the number of time-bins denoted by B, let $\mathbf{Z}$ be the $n \times B$ binned and z-scored spike-count matrix with element (i, b) equal to $z_{i,b}$. From this matrix $\mathbf{Z}$ assembly-patterns were identified in two steps: (1) the number of significant patterns in the data was estimated based on random matrix theory, after which (2) the corresponding number of assembly-patterns was extracted using ICA. Note that here a "pattern" is described by a weight vector over the n principal cells recorded that day. In the dataset used here the average number of principal cells was 30.11±2.51 per recording day.

Determination of the number of significant assembly-patterns—A principal component analysis was first applied to matrix $\mathbf{Z}$. The pairwise correlation matrix of $\mathbf{Z}$ is given by $\mathbf{C} = \frac{1}{n}\mathbf{Z}\mathbf{Z}^{\mathrm{T}}$ (where $\mathbf{Z}^{\mathrm{T}}$ is the transpose of $\mathbf{Z}$) and the eigenvalue-decomposition of $\mathbf{C}$ is given by:

$$\sum_{j=1}^{n}\lambda_j \boldsymbol{p}_j \boldsymbol{p}_j^{\mathrm{T}} = \mathbf{C}$$

where λ_j is the jth eigenvalue of $\mathbf{C}$ and $\boldsymbol{p}_j$ its corresponding eigenvector (i.e., principal component of $\mathbf{Z}$) (for $j = 1, \dots, n$). To estimate the number of significant patterns embedded within $\mathbf{Z}$, the Marčenko-Pastur distribution was used which states that the eigenvalues of the correlation matrix obtained from a $\mathbf{Z}$ matrix whose elements are independent and identically distributed random variables (with zero mean and unit variance) are asymptotically (i.e., when $n, B \to \infty$ such that B/n converges to a finite positive value) bounded to the interval $\left[\left(1 - \sqrt{n/B}\right)^2, \left(1 + \sqrt{n/B}\right)^2\right]$[35]. This implies that none of the eigenvalues of the correlation matrix of a $\mathbf{Z}$ matrix constructed from the spike trains of neurons with independent firing activity is expected to exceed $\lambda_{\max} = \left(1 + \sqrt{n/B}\right)^2$, as demonstrated elsewhere (for $B > n$)[36,37]. An eigenvalue above $\lambda_{\max}$ thus indicates that the pattern given by the corresponding principal component captures more correlation in the data than any pattern could if the firing activity of all neurons was independent. The number of eigenvalues above $\lambda_{\max}$ (denoted by N_A) therefore represents the minimum number of distinct significant patterns in the data[33,38].

Identification of assembly-pattern composition using ICA—The first N_A principal components each capture a significant amount of correlation between the firing patterns of the neurons. However, principal components are restricted to be orthogonal to each other while cell assemblies do not need to be (e.g., they can contain overlapping neurons). Principal components are also extracted from the data sequentially, which usually causes the first principal component to seemingly be a mixture of multiple assembly-patterns[36,39] (our own observation not shown). Moreover, principal component analysis is solely based on pairwise correlations while higher-order correlations can also inform assembly identification. To avoid these issues, ICA was used instead. The ICA extracts patterns such that the linear projections of the data onto these patterns are as independent from each other as possible. However ICA directly applied to **Z** without prior dimension reduction would extract as many patterns as there are neurons[33]. To restrict the number of patterns identified by ICA to N_A, the data was first projected onto the subspace spanned by the first N_A principal components:

$$Z_{\mathrm{PROJ}} = \mathbf{P}_{\mathrm{SIGN}}{}^{\mathrm{T}} Z$$

where $\mathbf{P}_{\mathrm{SIGN}}$ is the $n \times N_A$ matrix with the first N_A principal components as columns. ICA was then applied to the matrix $\mathbf{Z}_{\mathrm{PROJ}}$. That is, an $N_A \times N_A$ un-mixing matrix **W** was found such that the rows of the matrix $\mathbf{Y} = \mathbf{W}^{\mathrm{T}}\mathbf{Z}_{\mathrm{PROJ}}$ were as independent as possible. This optimization-problem was solved using the fast ICA algorithm[40,41]. The resulting un-mixing matrix **W** was then expressed in the original basis spanned by all the neurons:

$$\mathbf{V} = \mathbf{P}_{\mathrm{SIGN}} \mathbf{W}$$

where the columns of **V** (i.e., $\mathbf{v}_1, \ldots, \mathbf{v}_{N_A}$) are the *assembly-patterns*. As both the sign and the scale of the ICA output is arbitrary, all assembly-patterns were scaled to unit length (i.e., $\sum_{i=1}^{n} \mathbf{v}_k{}^2(i) = 1$) and their sign set such that the highest absolute weight of each pattern was always positive. The contribution of each neuron towards the temporal expression of an assembly-pattern was taken as its squared weight (25ms time-bins: Days 1-3: 436 and 1312 patterns; Days 4-6: 162 and 411 patterns; theta-cycle time-bins: Days 1-3: 380 and 1128 patterns; Days 4-6: 123 and 438 patterns; with tagged and alternative neurons, respectively).

Tracking the activation-strength of assembly-patterns over time—To determine whether the optogenetic manipulation altered the strength of the expressed assemblies, we tracked each assembly-pattern $\mathbf{v}_k$ over time by:

$$R_k(t) = z(t)^{\mathrm{T}} \mathbf{P}_k z(t)$$

where $z(t)$ is a smooth vector-function containing for each neuron its z-scored instantaneous firing-rate and $\mathbf{P}_k$ is the matrix projecting $z(t)$ to the activation-strength of assembly-pattern k at time t. $\mathbf{P}_k$ was taken as the outer product of $\mathbf{v}_k$ with the main diagonal entries set to zero to prevent high activation-strength caused by the isolated activity of a single neuron with

high weight to that pattern. With this approach, only interactions between neurons could contribute towards the activation-strength of an assembly-pattern[33,36–38]. To increase the temporal resolution beyond the bin-size used to identify the assembly-patterns, $z(t)$ was obtained by convolving the spike-train of each neuron with a kernel-function[33,42] after which the resulting smooth curve was normalized by a z-score transform. A Gaussian kernel was chosen with standard deviation $w/\sqrt{12}$, so that the kernel had the same standard deviation as fixed time-bins of w ms [43]. We set w to 25ms to match the bin-size used to identify the assembly-patterns. The resulting activation-strength time-courses showed a low baseline with sparse, transient peaks. Assembly-activations were defined as peaks exceeding $R_{\text{THRES}} = 5$ (Supplementary Fig. 9g,h).

Conditioned place preference (CPP)

The CPP apparatus consisted of a circle (46cm diameter, 38cm height) and a square (46cm×46cm×38cm) compartment connected *via* a bridge (8cm length, 5cm width), which was present during the Pre-test, the two CPP tests, the Extinction, the Drug-priming and the Novel sessions. All CPP experiments were performed using adult male mice and all days are numbered relative to the tagging day (Day 0; Figure 3a and Supplementary Fig. 11b). All mice were handled for at least 3 days prior to the experiment. On the first experiment day (Day -7), drug-free mice explored the entire apparatus for 15min to determine their baseline preference for one of the two compartments (Pre-test). Then, mice were conditioned for three days (Day -6, -5 and -4) with two pairing sessions each day. Conditioning was performed with respect to the initial preference of each animal (as identified during the Pre-test) for one of the two compartments[44,45]. In the first session, mice received saline (0.9% saline, i.p.) prior to exploring the preferred compartment for 20min (saline-paired compartment). In the second session, 5h later, mice received cocaine (10mg/kg, i.p.; Sigma) prior to exploring the least-preferred compartment for 20min (cocaine-paired compartment). On the day after (22h after) the last conditioning session the cocaine place memory was assessed by allowing (drug-free) mice to explore the entire apparatus for 15min (Test 1; Day -3). Dox was subsequently removed from the diet of tagged mice, but not control mice. Mice were injected with cocaine (10mg/kg, i.p.; Sigma) prior to re-exposure to the cocaine-paired compartment for the tagging procedure (45min; Day 0). Both tagged and control mice were put on high Dox immediately after, and on regular Dox the next day. During each one of the three following days (Days 1–3) mice were successively re-exposed to the saline-paired compartment without photo-silencing (20min exploration) and to the cocaine-paired compartment 5h later with ArchT photo-silencing (20min exploration). The locomotor behavior of control and tagged c-fos::ArchT mice during re-exposure to the cocaine-paired enclosure was similar (distance travelled = 48.51±3.32m versus 54.26±2.74m, animal speed = 4.04±0.27cm/s versus 4.52±0.23cm/s; P=0.18). The cocaine place memory was re-assessed by allowing mice to explore the entire apparatus for 15min (Test 2, Day 4). For each mouse the time spent in each compartment was measured during the pre-test and the two tests sessions and the cocaine place preference score calculated as the difference between the time spent in the cocaine-paired compartment minus that in the saline-paired compartment over their sum. Two additional experiments using the CPP apparatus were performed. The first was to test the ability of the mice to subsequently reinstate a cocaine place preference when cocaine-primed (10mg/kg, i.p.; Sigma; Supplementary Figure 11d)[46]

and the second was to test their ability to detect spatial novelty (Supplementary Figure 11e). Because control mice exhibited a cocaine place preference in Test 2 (see Figure 3c), we used a trial-to-criterion approach to extinguish their place preference prior to the drug-primed reinstatement test by repeatedly testing their place preference until their CPP score was no more than 0.04 (number of additional tests: 3.50±0.88)[46]. The drug-priming test was performed 24 hours after the extinction criterion was reached for control mice or 24h after Test 2 for tagged mice, then followed by the spatial novelty test. For each mouse the time spent in each compartment was measured during both the drug-priming and the novelty tests. The cocaine place preference score was calculated as mentioned above, and the novel place preference was scored by the time spent in the new compartment minus that in the other (familiar) compartment over their sum.

Cocaine place memory retrieval in c-fos-tTA-LacZ mice

A group of c-fos-tTA-LacZ adult male mice was used to evaluate the extent to which dorsal CA1 neurons that were activated during the exploration of the tagged open-field enclosure associated with a cocaine (n=7 mice) or a saline (n=4 mice) administration were subsequently re-activated during a (drug-free) spatial context re-exposure (Supplementary Fig. 10). Mice were individually housed for at least two weeks (and regular Dox was removed three days) before the tagging day. The tagging day consisted of injecting mice with either saline (0.9% saline, i.p.) or cocaine (10mg/kg, i.p.; Sigma) before they were allowed to explore the open-field enclosure for 30min. A high dose of Dox (1g/kg) was provided immediately after the exploration session before returning to regular Dox one day after. Drug-free mice were re-exposed to the tagged enclosure three days later and perfused 90min after. Brains were extracted for immunohistochemistry procedures (Supplementary Figure 10).

Tissue processing and immunohistochemistry

At the completion of the experiments all mice were deeply anesthetized with pentobarbital and transcardially perfused with 0.1M phosphate buffer saline (PBS) followed by cold 4% paraformaldehyde (4% PFA) dissolved in PBS[24]. Brains were extracted and kept in 4% PFA for at least 24h before slicing and sections were stored in PBS-azide. For immunostaining, free-floating sections were rinsed extensively in PBS with 0.25% Triton X-100 (PBS-T) and were blocked for 1h at room temperature in PBS-T with 10% normal donkey serum (NDS). Sections were then incubated with primary antibodies diluted in 3% NDS blocking solution and incubated at 4°C for 72h (rabbit polyclonal anti-neuropeptide tyrosine NPY 1:1,500, Abcam; goat polyclonal anti-Parvalbumin PV 1:4,000, Swant; rat monoclonal anti-Somatostatin 1:1,000; mouse monoclonal anti-beta-Galactosidase 1:10,000, Promega; rabbit polyclonal anti-c-Fos 1:10,000, Santa Cruz). All sections were rinsed three times for 15min in PBS-T and incubated for 4h at room temperature in secondary antibodies (Jackson ImmunoResearch; donkey anti-rat AMCA 1/250; donkey anti-rabbit Cy3 1/1,000; donkey anti-mouse 647 1/500; donkey anti-goat 647, 1/500) diluted in the blocking solution. This step was followed by three rinses for 15min in PBS-T. Sections were then incubated for 1min with 4′, 6-diamidino-2-phenylindole (Dapi, 0.5µg/ml, Sigma, D8417) diluted in PBS to label cell nuclei before undergoing three additional rinse steps of 10min each in PBS.

Sections were mounted on slides, cover-slipped with Vectashield mounting medium (Vector Laboratories, CA) and stored at 4°C.

Image acquisition and quantification

Images shown in Figure 1c and Supplementary Figure 10c were acquired using a laser-scanning confocal microscope (LSM 710; Zeiss, 40×/1.3 objective) in sequential scanning mode. A single 1μm confocal plane was used for Dapi pictures with flattened *z*-stacks (2μm step) for the GFP, LacZ or Fos signals. Series of tiled single-plan GFP and Dapi images shown in Supplementary Figure 1b were acquired using an epifluorescence microscope (AxioImager M2; Zeiss, 10×/0.45 objective) and StereoInvestigator software (Virtual Tissue 2D module, MBF Bioscience). Counting was performed on z-stacks using StereoInvestigator (MBF Bioscience) and ImageJ (http://rsb.info.nih.gov/) software. An experimenter blind to each condition outlined the pyramidal cell layer of the dorsal CA1 according to the Dapi signal in each brain section. The experimenter estimated the total number of Dapi positive cells in the CA1 pyramidal cell layer by randomly outlining 9 CA1 sample areas on sections from a subset of c-fos::ArchT mice (n=3). In Figure 1, quantification of ArchT-GFP positive neurons in the pyramidal cell layer was conducted from 1-in-3 coronal sections (50μm thickness, average of n=11.14±1.31 CA1 hippocampi per mouse) throughout the dorsal CA1 (−1.46 to −2.46mm from bregma) from tagged (n=4) and control (n=3) mice perfused on Day3. In each hippocampus section, the percentage of ArchT-GFP cells expressing the different interneuron markers (Parvalbumin PV, neuropeptide-Y NPY and somatostatin) was evaluated. Putative pyramidal cells were required to exhibit dendritic spines (Figure 1c) and be immunonegative for PV, NPY and somatostatin, markers known to capture interneurons[27,28,47,48]. In Supplementary Fig. 10, quantification of LacZ-positive and Fos-positive neurons in the pyramidal cell layer was conducted from 1-in-7 coronal sections (30μm thickness, average of n=11.91±0.45 CA1 hippocampi per mouse) throughout the dorsal CA1 (−1.31 to −2.53 from bregma) from saline (n=4) and cocaine (n=7) mice.

Statistical analysis

Data are presented as mean ± standard error of the mean. All P values were calculated in R (www.r-project.org) using a two-sided *t*-test or an ANOVA followed by a *post-hoc* Tukey's test for multiple comparisons, unless specified otherwise.

Supplementary Material

Refer to Web version on PubMed Central for supplementary material.

Acknowledgments

References

1. Schacter DL, Addis DR, Buckner RL. Nat. Rev. Neurosci. 2007; 8:657–661. [PubMed: 17700624]

2. O'Keefe J, Dostrovsky J. Brain Res. 1971; 34:171–175. [PubMed: 5124915]

3. Wilson MA, McNaughton BL. Science. 1993; 261:1055–1058. [PubMed: 8351520]

4. Leutgeb S, et al. Science. 2005; 309:619–623. [PubMed: 16040709]

5. Buzsáki G. Neuron. 2010; 68:362–385. [PubMed: 21040841]

6. Robbins TW, Ersche KD, Everitt BJ. Ann. N. Y. Acad. Sci. 2008; 1141:1–21. [PubMed: 18991949]

7. Muller RU, Kubie JL. J. Neurosci. Off. J. Soc. Neurosci. 1987; 7:1951–1968.

8. Bostock E, Muller RU, Kubie JL. Hippocampus. 1991; 1:193–205. [PubMed: 1669293]

9. Leutgeb S, Leutgeb JK, Treves A, Moser M-B, Moser EI. Science. 2004; 305:1295–1298. [PubMed: 15272123]

10. Kelemen E, Fenton AA. PLoS Biol. 2010; 8:e1000403. [PubMed: 20585373]

11. Wills TJ, Lever C, Cacucci F, Burgess N, O'Keefe J. Science. 2005; 308:873–876. [PubMed: 15879220]

12. Lee I, Yoganarasimha D, Rao G, Knierim JJ. Nature. 2004; 430:456–459. [PubMed: 15229614]

13. Thompson LT, Best PJ. J. Neurosci. 1989; 9:2382–2390. [PubMed: 2746333]

14. Epsztein J, Brecht M, Lee AK. Neuron. 2011; 70:109–120. [PubMed: 21482360]

15. Karlsson MP, Frank LM. J. Neurosci. 2008; 28:14271–14281. [PubMed: 19109508]

16. Mizuseki K, Buzsáki G. Cell Rep. 2013; 4:1010–1021. [PubMed: 23994479]

17. Lee D, Lin B-J, Lee AK. Science. 2012; 337:849–853. [PubMed: 22904011]

18. Hirase H, Leinekugel X, Czurkó A, Csicsvari J, Buzsáki G. Proc. Natl. Acad. Sci. U. S. A. 2001; 98:9386–9390. [PubMed: 11470910]

19. Ramirez S, et al. Science. 2013; 341:387–391. [PubMed: 23888038]

20. Redondo RL, et al. Nature. 2014; 513:426–430. [PubMed: 25162525]

21. Drane L, Ainsley JA, Mayford MR, Reijmers LG. Front. Mol. Neurosci. 2014; 7:82. [PubMed: 25400545]

22. Reijmers LG, Perkins BL, Matsuo N, Mayford M. Science. 2007; 317:1230–1233. [PubMed: 17761885]

23. Han X, et al. Front. Syst. Neurosci. 2011; 5:18. [PubMed: 21811444]

24. McNamara CG, Tejero-Cantero Á, Trouche S, Campo-Urriza N, Dupret D. Nat. Neurosci. 2014; 17:1658–1660. [PubMed: 25326690]

25. Csicsvari J, Hirase H, Czurkó A, Mamiya A, Buzsáki G. J. Neurosci. Off. J. Soc. Neurosci. 1999; 19:274–287.

26. Harris KD, Henze DA, Csicsvari J, Hirase H, Buzsáki G. J. Neurophysiol. 2000; 84:401–414. [PubMed: 10899214]

27. Lapray D, et al. Nat. Neurosci. 2012; 15:1265–1271. [PubMed: 22864613]

28. Katona L, et al. Neuron. 2014; 82:872–886. [PubMed: 24794095]

29. Varga C, et al. eLife. 2014; 3

30. Dupret D, O'Neill J, Pleydell-Bouverie B, Csicsvari J. Nat. Neurosci. 2010; 13:995–1002. [PubMed: 20639874]

31. Muller RU, Kubie JL. J. Neurosci. Off. J. Soc. Neurosci. 1989; 9:4101–4110.

32. O'Neill J, Senior TJ, Allen K, Huxter JR, Csicsvari J. Nat. Neurosci. 2008; 11:209–215. [PubMed: 18193040]

33. Lopes-dos-Santos V, Ribeiro S, Tort ABL. J. Neurosci. Methods. 2013; 220:149–166. [PubMed: 23639919]

34. Harris KD, Csicsvari J, Hirase H, Dragoi G, Buzsáki G. Nature. 2003; 424:552–556. [PubMed: 12891358]

35. Mar enko VA, Pastur LA. Math USSR-Sbornik. 1967; 1:457–83.

36. Lopes-dos-Santos V, Conde-Ocazionez S, Nicolelis MAL, Ribeiro ST, Tort ABL. PloS One. 2011; 6:e20996. [PubMed: 21698248]

37. Peyrache A, Benchenane K, Khamassi M, Wiener SI, Battaglia FP. J. Comput. Neurosci. 2010; 29:309–325. [PubMed: 19529888]

38. Peyrache A, Khamassi M, Benchenane K, Wiener SI, Battaglia FP. Nat. Neurosci. 2009; 12:919–926. [PubMed: 19483687]

39. Laubach M, Shuler M, Nicolelis MA. J. Neurosci. Methods. 1999; 94:141–154. [PubMed: 10638821]

40. Hyvärinen A. IEEE Trans. Neural Netw. Publ. IEEE Neural Netw. Counc. 1999; 10:626–634.

41. Marchini, JL.; Heaton, C.; Ripley, BD. 2013. at <http://cran.r-project.org/package=fastICA.>

42. Dupret D, O'Neill J, Csicsvari J. Neuron. 2013; 78:166–180. [PubMed: 23523593]

43. Kruskal PB, Stanis JJ, McNaughton BL, Thomas PJ. Stat. Med. 2007; 26:3997–4008. [PubMed: 17593566]

44. Meyers RA, Zavala AR, Neisewander JL. Neuroreport. 2003; 14:2127–2131. [PubMed: 14600510]

45. Dela Cruz AM, Herin DV, Grady JJ, Cunningham KA. Behav. Pharmacol. 2009; 20:720–730. [PubMed: 19901823]

46. Aguilar MA, Rodríguez-Arias M, Miñarro J. Brain Res. Rev. 2009; 59:253–277. [PubMed: 18762212]

47. Somogyi P, Katona L, Klausberger T, Lasztóczi B, Viney TJ. Philos. Trans. R. Soc. Lond. B. Biol. Sci. 2014; 369:20120518. [PubMed: 24366131]

48. Viney TJ, et al. Nat. Neurosci. 2013; 16:1802–1811. [PubMed: 24141313]

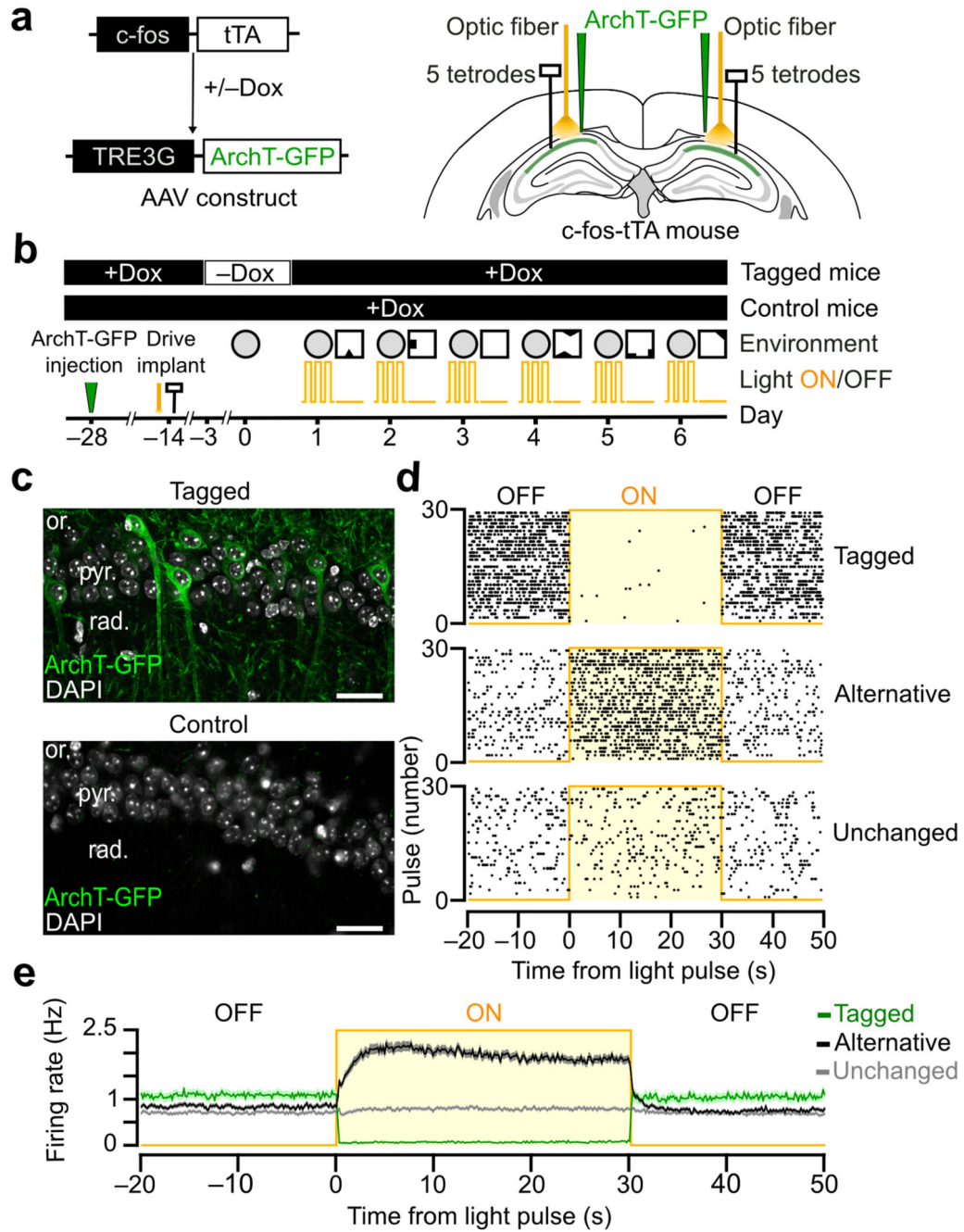**Figure 1. Activity-dependent tagging of CA1 neurons**
(a) c-fos-tTA mice were bilaterally injected with a TRE3G-ArchT-GFP virus and implanted with tetrodes and optic fibers in the dorsal CA1. (b) c-fos::ArchT tagged, but not c-fos::ArchT control, mice were transiently taken off Dox to tag CA1 neurons recruited in the circle with tTA-TRE3G interaction-driven ArchT expression. Ensemble recordings and light-delivery were performed in subsequent days in the circle and square enclosures. (c) ArchT-GFP expressing neurons in the pyramidal cell layer of a tagged, but not a control, mouse. Stratum oriens (or.), pyramidale (pyr.), radiatum (rad.). Cell nuclei stained with

Dapi. Scale bars: 30μm. **(d)** Raster plots showing spike times relative to 30s light-pulses for three neurons simultaneously recorded from the same tetrode. The top (1.59Hz versus 0.01Hz) but not the bottom (0.43Hz versus 0.40Hz) neuron was photo-silenced whereas the middle neuron increased its firing (0.38Hz versus 1.51Hz). **(e)** Firing rate light-response (mean±s.e.m) of all CA1 principal neurons recorded and grouped according to their light-modulation (as in **d**).
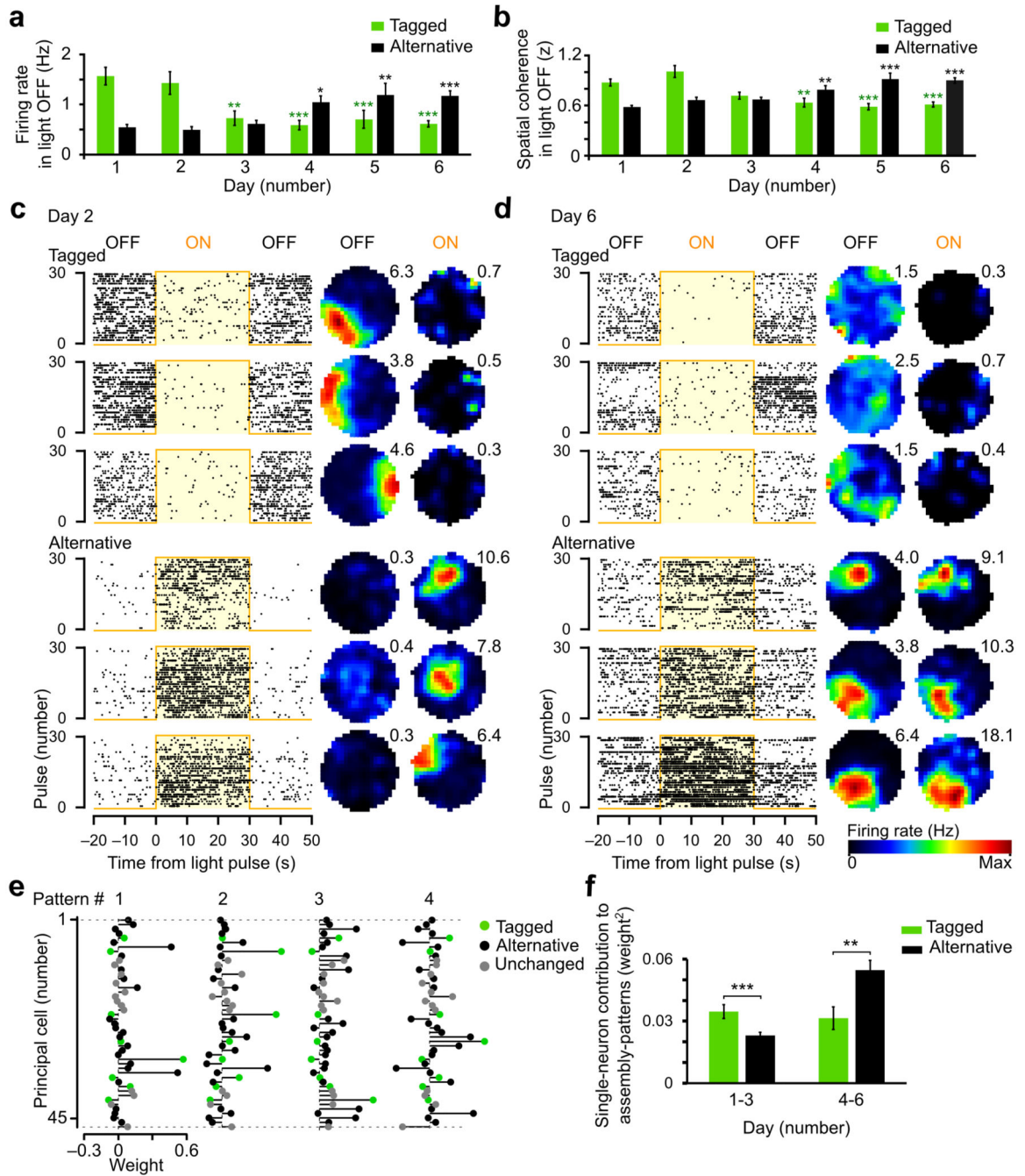
Figure 2. Photo-silencing of tagged neurons enabled alternative neurons to emerge and provide an alternative map

(a,b) Baseline (light-OFF) firing rate (a) and spatial coherence (b) of tagged and alternative neurons from tagged mice exploring the circle (mean±s.e.m). *P<0.05, **P<0.01, ***P<0.001: comparison to Day 1. (c,d) Example raster plots and spatial rate maps of simultaneously recorded neurons on Day 2 (c) and Day 6 (d). Distinct neurons were recorded on each day; one cell per row. Spatial rate maps are scaled to the peak firing rate (Hz; top right of each map) or 1Hz for low-firing cells. Warm colors (red) correspond to the

cell's place field. **(e)** Example weight vectors representing simultaneously recorded assembly-patterns detected from 25ms co-fluctuation of (light-OFF) spike discharge in the circle. **(f)** Average single-neuron contribution to the temporal expression of assembly-patterns during the first and the second three-day blocks using 25-ms time windows (mean ±s.e.m). **P<0.01, ***P<0.001.
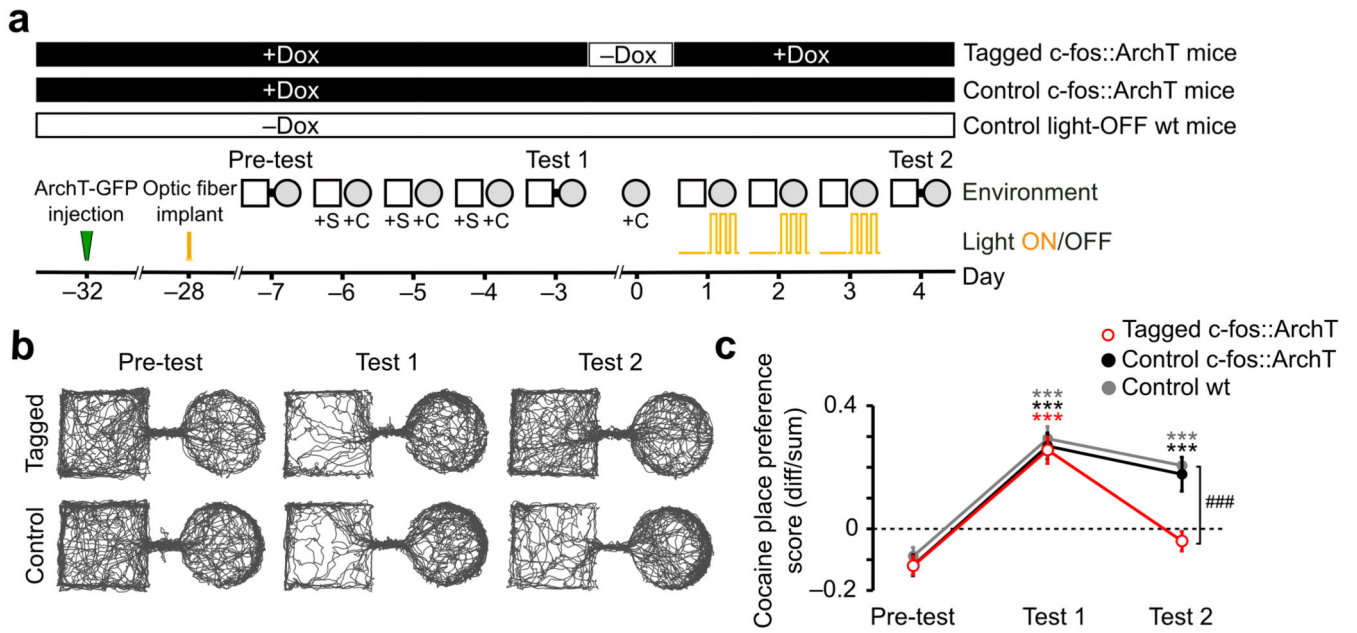
Figure 3. CA1 photo-recoding revoked an otherwise long-lasting cocaine-place memory
(a) Cocaine-conditioned place preference paradigm. Mice explored the entire apparatus
(Pre-test) before the preferred compartment was paired with saline (+S) and the other with
cocaine (+C) administration, followed by a place-preference test (Test 1). Then tagged, but
not control, c-fos::ArchT mice were transiently taken off Dox to tag active CA1 neurons and
all mice received cocaine in the cocaine-paired compartment. CA1 light was delivered to all
c-fos::ArchT mice during subsequent (drug-free) re-exposure to the cocaine-paired
compartment, followed by a second place-preference test (Test 2). (b) Example paths for c-
fos::ArchT tagged and control mice during Pre-test, Test 1 and Test 2. (c) Cocaine-place
preference score (mean±s.e.m). During each test drug-free mice had access to the entire
apparatus and their place preference was scored as the difference between the time spent in
the cocaine-paired compartment minus that in the saline-paired compartment over their sum.
Within-group comparison to Pre-test: ***P<0.001. Test 2, between-group comparison:
###P<0.001.